Metalloprotein Crystallography: More than a Structure

Citation: Bowman, Sarah E. J., Jennifer Bridwell-Rabb, and Catherine L. Drennan. "Metalloprotein Crystallography: More than a Structure." Accounts of Chemical Research 49.4 (2016): 695–702. © 2016 American Chemical Society

As Published: http://dx.doi.org/10.1021/acs.accounts.5b00538

Publisher: American Chemical Society (ACS)

Persistent URL: http://hdl.handle.net/1721.1/110463

Version: Final published version: final published article, as it appeared in a journal, conference proceedings, or other formally published context

ACCOUNTS of chemical research

Article

pubs.acs.org/accounts

Metalloprotein Crystallography: More than a Structure

Sarah E. J. Bowman,[†,§,⊥] Jennifer Bridwell-Rabb,[†,‡,§,⊥] and Catherine L. Drennan*[,†,‡,§]

[†]Department of Chemistry, [‡]Department of Biology, and [§]Howard Hughes Medical Institute, Massachusetts Institute of Technology, 77 Massachusetts Avenue, Cambridge, Massachusetts 02139, United States

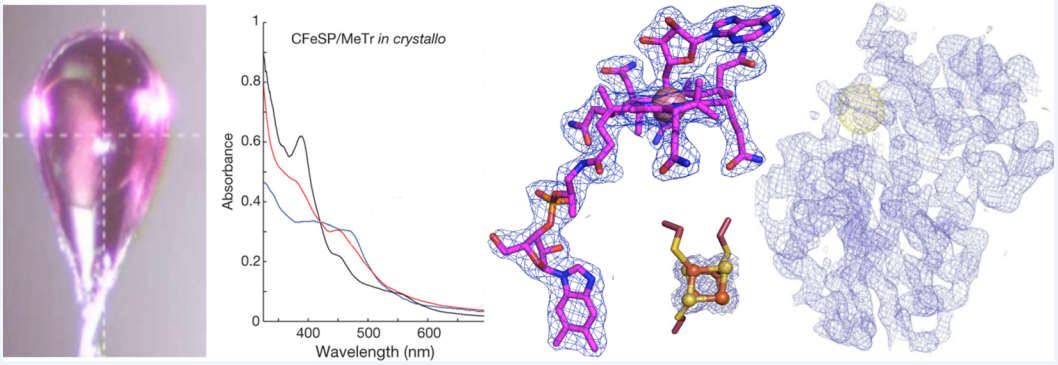

CONSPECTUS: Metal ions and metallocofactors play important roles in a broad range of biochemical reactions. Accordingly, it has been estimated that as much as 25−50% of the proteome uses transition metal ions to carry out a variety of essential functions. The metal ions incorporated within metalloproteins fulfill functional roles based on chemical properties, the diversity of which arises as transition metals can adopt different redox states and geometries, dictated by the identity of the metal and the protein environment. The coupling of a metal ion with an organic framework in metallocofactors, such as heme and cobalamin, further expands the chemical functionality of metals in biology. The three-dimensional visualization of metal ions and complex metallocofactors within a protein scaffold is often a starting point for enzymology, highlighting the importance of structural characterization of metalloproteins. Metalloprotein crystallography, however, presents a number of implicit challenges including correctly incorporating the relevant metal or metallocofactor, maintaining the proper environment for the protein to be purified and crystallized (including providing anaerobic, cold, or aphotic environments), and being mindful of the possibility of X-ray induced damage to the proteins or incorporated metal ions. Nevertheless, the incorporated metals or metallocofactors also present unique advantages in metalloprotein crystallography. The significant resonance that metals undergo with X-ray photons at wavelengths used for protein crystallography and the rich electronic properties of metals, which provide intense and spectroscopically unique signatures, allow a metalloprotein crystallographer to use anomalous dispersion to determine phases for structure solution and to use simultaneous or parallel spectroscopic techniques on single crystals. These properties, coupled with the improved brightness of beamlines, the ability to tune the wavelength of the X-ray beam, the availability of advanced detectors, and the incorporation of spectroscopic equipment at a number of synchrotron beamlines, have yielded exciting developments in metalloprotein structure determination. Here we will present results on the advantageous uses of metals in metalloprotein crystallography, including using metallocofactors to obtain phasing information, using K-edge X-ray absorption spectroscopy to identify metals coordinated in metalloprotein crystals, and using UV−vis spectroscopy on crystals to probe the enzymatic activity of the crystallized protein.

INTRODUCTION

The chemical versatility of transition metals leads to their essential roles in enzymatic systems. It has been estimated that 25−50% of all proteins found within an organism contain metal ions.[1,2] In a systematic assessment of protein structures deposited in the PDB at the time of this Account, of the 99 827 structures determined using X-ray crystallography, 21 989 contain transition metals or metallocofactors. Therefore, approximately 22% of protein structures deposited in the PDB contain biologically relevant d-block transition metals or cofactors such as heme, iron−sulfur (Fe−S) cluster, and cobalamin (Cbl), which establishes a lower bound to the number of proteins in the proteome that coordinate metals. Once incorporated within enzymes, metal ions expand the catalytic repertoire of enzymes. For example, iron plays roles in electron transfer, radical chemistry, and activation of oxygen, nickel functions in biological carbon, nitrogen, and oxygen cycles, copper is important in electron transport and oxidation−reduction reactions, and zinc plays roles in maintaining protein structure or acting as a Lewis acid to facilitate chemistry.[3]

This diversity of function comes at a price, because almost all free transition metal ions are toxic when in excess; organisms

Received: December 11, 2015
Published: March 15, 2016

DOI: 10.1021/acs.accounts.5b00538
Acc. Chem. Res. 2016, 49, 695−702

must strictly regulate metal ion uptake, use, and export, and must ensure that the correct metal is incorporated into the correct protein. Metallochaperones are often employed during metallocofactor biosynthesis, protecting organisms from toxic effects of free cofactors or their building blocks.[4] To these ends, elaborate multicomponent Fe−S cluster assembly systems have evolved for maturation and delivery of Fe−S cluster cofactors.[5] Likewise, specialized systems are required for the maturation and assembly of the catalytic H cluster in Fe−Fe hydrogenase,[6] the biosynthesis and insertion of the P-cluster and iron molybdenum cofactor (FeMoco) of nitrogenase,[7] and the maturation of the nickel-containing C-cluster of the *Rhodospirillum rubrum* carbon monoxide dehydrogenase (CODH).[8]

Crystal structures determined from data collected using synchrotron radiation provide high-resolution snapshots of biomolecules. Improvements at beamlines, including higher brightness, flux, and availability of advanced detectors, has led to better quality data and higher-resolution crystal structures. A notable example of these improvements is the structure that resolved the identity of the light atom in nitrogenase, the enzyme that converts atmospheric nitrogen to ammonia. The original 2.2 Å resolution structure of nitrogenase detailed an FeMoco with a geometrically complex arrangement of six inner iron atoms and nine surface sulfur atoms.[9] This arrangement of identical scatterers resulted in additive ripple effects from each atom, effectively concealing the central light atom and leading to the initial incorrect interpretation of an empty pocket.[10] In a later 1.16 Å resolution structure, a light atom at the center of the FeMoco was observed but unable to be unambiguously assigned.[11] The light atom X was speculated to be carbon, nitrogen, or oxygen, which led to a broad range of proposed mechanisms.[11,12] The correct identification of atom X was the focus of much scientific investigation (and heated debate). The recently solved 1.0 Å resolution structure allowed for clear identification of X as a carbon atom.[13]

Concomitant with improvements available from brighter synchrotron sources are the potentially damaging effects of X-ray radiation. These deleterious effects are of special concern in biomolecules containing transition metals because these atoms are often more susceptible to radiation damage and oxidation state changes. Using multiple methods to investigate structural questions has the advantage of providing complementary information and additional insight into function and mechanism. The power of using different experimental techniques can be observed by revisiting the nitrogenase mystery. In addition to higher resolution crystallographic data, assignment of X to carbon was confirmed using electron spin echo envelope modulation studies.[13] An independent spectroscopic study using X-ray emission spectroscopy also identified the central X atom as carbon.[14] Using parallel spectroscopic techniques on solution and crystal samples can determine whether a crystallographically observed conformation of an enzyme is an active or inactive state.[15] Combining crystallography with *in crystallo* spectroscopic techniques can yield large amounts of information. Early examples include identification of X-ray damage to the Mn_4Ca complex in photosystem II[16] and assignment of individual iron oxidation states in the [2Fe−2S] clusters of ferredoxin crystals using X-ray absorption (XAS).[17] A variety of spectroscopic techniques have since been incorporated into equipment available at synchrotron beamlines to both assess potential synchrotron radiation difficulties and gain insight into the mechanisms of metalloproteins with crystallographically determined structures (Table 1).[18,19]

Table 1. Techniques Available at Macromolecular Crystallographic Diffraction Data Collection Beamlines[a]

country	synchrotron	beamline	technique
Canada	Canadian Light Source	CMCF-BM	EDX, XANES, EXAFS
		CMCF-1D	EDX, XANES
China	Beijing Synchrotron Radiation Facility	1W2B	EDX, EXAFS
France	European Synchrotron Radiation Facility	ID29S	UV−vis, fluorescence, Raman (offline)
		ID29	Raman
Japan	Spring-8	BL38B1	UV−vis
Switzerland	Swiss Light Source	X10SA	UV−vis, resonance Raman
United Kingdom	Diamond Light Source	MX 102, 103, 104 and 124	UV−vis
United States	Advanced Photon Source	14-BM-C	UV−vis
		21-ID-D	EDX
		24-ID-E, 24-ID-C	EDX
	Stanford Synchrotron Radiation Lightsource	9-2	UV−vis, EDX, Raman
		11-1	UV−vis, EDX
		9-1, 12-2	EDX

[a]As indicated on their websites. Some of the beamlines could have additional unlisted capabilities.

Microspectrophotometry on metalloprotein crystals can yield information about the metal redox state(s), identify which metals and cofactors are present, and assess radiation damage caused by the X-ray beam.[20−22] Techniques that take advantage of K-edge absorption energies, of particular use in characterizing spectroscopically silent metals, include energy dispersive emission line scans (EDX), which can identify what metals are present, and X-ray absorption near edge structure (XANES) and extended X-ray absorption fine structure (EXAFS), both of which can identify redox state changes and provide geometric constraints for structural refinement.[17,18,23] Resonance Raman on single crystals provides information about redox state changes and metal−ligand interactions.[24,25] These techniques have been utilized on single crystals in parallel and simultaneous modes, before, during, and after X-ray data collection, in a variety of cases in which the spectroscopy has led to a better understanding of the structural results. Development of equipment at synchrotron sources that allows for concurrent spectroscopic data has been exploding, and in this Account, we discuss examples of the types of information that can be obtained from a range of available *in situ* synchrotron techniques for investigating metalloprotein crystals.

CHALLENGES OF METALLOPROTEIN CRYSTALLOGRAPHY

Protein Preparation

There are additional challenges in preparing samples for metalloprotein crystallography, because the correct metal center must be incorporated into the protein. In some cases, samples can be purified from the native organism containing the correct metal ion or metallocofactor, as exemplified by nitrogenase from *Azotobacter vinelandii*,[26] corrinoid Fe−S protein (CFeSP) from *Moorella thermoacetica*,[15] and *R. rubrum* CODH.[27] Alternatively, BtrN[28] and anSME[29] are examples of enzymes that have been purified recombinantly in *Escherichia*

DOI: 10.1021/acs.accounts.5b00538
Acc. Chem. Res. 2016, 49, 695−702

coli with intact [4Fe−4S] clusters through coexpression with the Fe−S cluster assembly operon (*isc*) from *A. vinelandii*.[5] Similarly, coexpression of the hydrogenase maturation genes (*hydEF*, *hydG*, and *hydA*) in *E. coli* leads to formation of an active Fe−Fe hydrogenase.[6]

In other cases, crystallization has been successful after anaerobic reconstitution of [4Fe−4S] clusters before crystallization,[30] through copurification from *E. coli* with an intact [4Fe−4S] cluster,[31] or using a combination of the *isc* operon and anaerobic reconstitution.[32] Excitingly, a structure of the Fe−Fe hydrogenase was recently determined in the presence of a semisynthetic H-cluster.[33] These additional steps to correctly reconstitute proteins for crystallography should be accompanied by complementary techniques to ensure correct incorporation.

Metalloprotein Crystallization

Metallocofactors including Fe−S clusters, FeMoco, and the H-cluster are notoriously susceptible to oxygen-induced degradation,[34] whereas the adenosylcobalamin (AdoCbl) cofactor is sensitive to light; both require special handling (Figure 1).

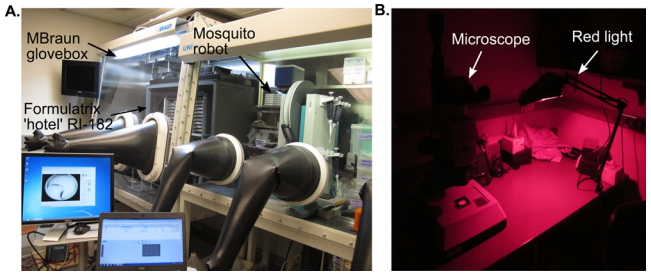

Figure 1. Anaerobic and aphotic crystallization setups. (A) Setup for metalloprotein crystallization under anaerobic conditions in an MBraun glovebox. Screens can be set up on the mosquito robot; crystal trays are stored and automatically imaged in the Formulatrix RI-182 within a custom designed chamber (Rebekah Bjork, Drennan Laboratory). (B) Light sensitive crystals are imaged and looped in a dark room equipped with red light.

For a protein with an active site metal center rather than a metallocluster, there are two methods for incorporating the metal of interest: soaking and cocrystallization. The structure of NikR, determined after soaking crystals with 8 mM nickel chloride, revealed 22 low-affinity nickel sites.[35] Here, cocrystallization was not an option because NikR precipitated when mixed with high nickel concentrations prior to crystallization.[35] Likewise, cocrystallization of the GTPase YjiA with Zn^{2+} was unsuccessful; therefore apo-YjiA crystals were grown and then soaked in a solution containing excess zinc sulfate.[36] For SyrB2, which requires an oxygen-sensitive Fe^{2+} center, crystals were grown aerobically and then transferred into an anaerobic chamber for soaking.[37]

X-ray Induced Changes to Metal Centers

Radiation damage to crystals is caused by X-ray generated free radicals. The diffusion rate of free radical species is reduced significantly at low temperature, and therefore X-ray experiments are performed with samples held at 100 K.[38] In the 1990s, it was estimated that the "lifetime" of a frozen crystal in the X-ray beam at a synchrotron was about 1 day.[39] Today, with the advent of third-generation synchrotrons, the predicted lifetime of a crystal at cryogenic temperatures is ∼5 min (the time it takes to collect one data set).[40,41] During data collection, at a wavelength of 1 Å, it is estimated that ∼10% of the X-ray photons exposed to a sample are elastically scattered and contribute useful information to structure determination.[42] This phenomenon means that the remaining 90% of photons will deposit their energy into the crystal, possibly causing global or specific damage.[42] Global damage is reflected in increased B-factors, higher mosaicity, higher R_{sym}, and lower resolution, whereas specific damage results in disulfide bond breaks, cysteine and methionine side chain oxidation, decarboxylation of acidic residues, or phenylalanine and tyrosine hydroxylation.[40,42] For metalloproteins, radiation damage can additionally lead to photoreduction.[20]

Redox state changes can impact the interpretation of metalloprotein crystal structures. For example, XAS experiments were performed on a series of free and protein-bound Cbl samples. The spectra of Co(II)−Cbl, methylcobalamin, and AdoCbl were similar before and after X-ray exposure.[43] The spectra of aquocobalamin and cyanocobalamin, however, were substantially altered by exposure to irradiating energies.[43] In another example, a series of crystal structures were solved for variants of cytochrome *c* (cyt *c*), a heme-containing protein from *Nitrosomonas europea* that functions in electron transfer reactions.[44] Previous EPR data of the variants showed differences in the heme electronic state.[45] Here, crystal structures were determined for the variants to correlate structural changes to electronic changes. The crystallographic analysis revealed some evidence of structural changes of the heme active site. Concomitant UV−vis data collected on protein crystals are consistent with Fe^{3+}-cyt *c* prior to X-ray exposure (the EPR active state) and Fe^{2+}-cyt *c* after data collection (Figure 2). These results may indicate that reduction of Fe^{3+} induces changes in both the heme electronic structure and observed Fe−ligand distance, factors that need to be considered when interpreting crystallographic results. An exquisite set of experiments was performed on cytochrome *c* peroxidase (CCP), another heme protein, to investigate the

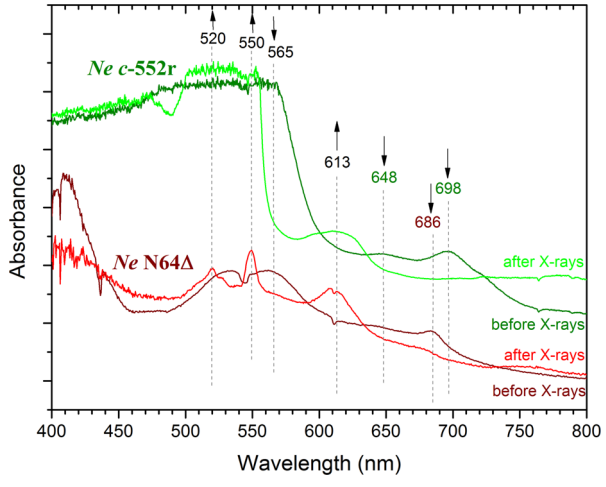

Figure 2. The X-ray beam causes reduction of the bound metallocofactor highlighting the importance of parallel techniques in metalloprotein crystallography. Characteristic bands indicate a low-spin Fe^{3+} state prior to X-ray exposure; appearance of the 613 nm band postexposure suggests some high-spin Fe^{2+}, consistent with ligand loss.[44] In the *Ne*N64D variant, low-spin Fe^{3+} is reduced to low-spin Fe^{2+}, evidenced by Q-bands at 520 and 550 nm.[44] Reproduced with permission from ref 44. Copyright 2013 Wiley-VCH Verlaf GmbH&Co, KGaA, Weinheim.

DOI: 10.1021/acs.accounts.5b00538
Acc. Chem. Res. 2016, 49, 695−702

molecular nature of Compound I.[46] In CCP crystal structures, the observed Fe−O bond length was ∼1.9 Å, significantly different from the bond lengths of 1.7 Å observed using spectroscopic methods. The shorter distance is consistent with an Fe(IV)═O species, whereas the longer distance is consistent with a protonated Fe(IV)−OH species. To examine whether the X-ray beam was correlated with lengthening the Fe−O bond, single-crystal spectroscopy and X-ray diffraction data were collected on ∼100 crystals, with a data collection strategy that allowed only brief exposure of each crystal to the X-ray beam.[46] These results showed the Fe−ligand bond length increases as a function of X-ray exposure, indicating previous X-ray structures had a mixed population of iron species, explaining the longer observed Fe−O bond lengths, and suggesting the longer bond length is an artifact caused by X-ray exposure.[46]

Crystallographic Refinement of Metal Centers

When the structure of a metal center is not known prior to the metalloprotein structure determination, care must be taken in how the metal site is refined.[23] Crystallographic parameters, such as bond lengths and angles, are well-established for proteins, but not for metal sites, and there is not a universally accepted strategy for refinement of metal centers.[1] Some crystallographers do not use distance or angle restraints when refining a metal site, afraid to bias the resulting structure. With high resolution data, this approach can work, but with modest resolution, this method can be dangerous. For example, refinement protocols are designed to alleviate clashes caused by atoms that are closer together than their van der Waals radii. Since most metal−ligand distances are shorter than this (2.2 Å is a typical Fe−cysteine distance), refinement can push apart atoms that should be close, biasing the resulting structure. For this reason, other crystallographers restrain metal−protein distances, using values from spectroscopy, from small molecule structures, or from other related metalloprotein structures. A general rule of thumb is that if you are not losing sleep over the refinement of the metal center, you are not being careful enough.

■ ADVANTAGES OF METALLOPROTEINS

The wealth of information and surprises revealed by metalloprotein crystallography outweigh its challenges. For example, the crystal structure of the non-heme iron halogenase SyrB2, which catalyzes the Fe^{2+}/α-ketoglutarate-dependent halogenation of threonine to 4-chloro-threonine using oxygen and chloride as substrates, revealed an unprecedented iron coordination to a chloride ion (Figure 3).[37] Importantly, this structure provided insight into how SyrB2 uses an Fe^{2+}/α-ketoglutarate-dependent enzyme scaffold that traditionally catalyzes hydroxylation reactions to instead catalyze halogenation.[37] In other cases, metalloprotein crystal structures have served as inspiration for synthetic chemists because they permit the molecular visualization of complicated metallocofactors. Since many metals have rich electronic properties that provide intense, spectroscopically unique signatures, spectroscopic characterization of metalloprotein crystals can provide detailed information about the metal site. Proteins that contain metals with strong absorption signals are ideally suited for parallel experiments; optical properties of a small subset of metalloproteins are listed in Table 2.

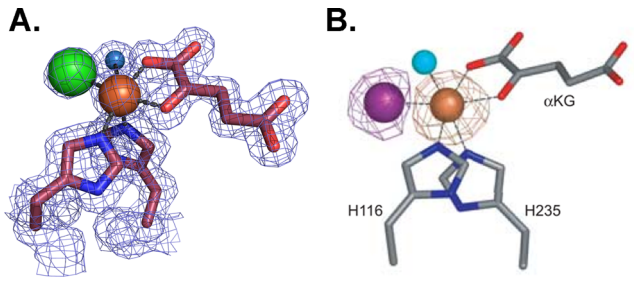

Figure 3. Crystal structure of SyrB2 provides insight into the halogenation mechanism. (A.) Active site of SyrB2, detailing an octahedral iron (brown sphere) geometry with two histidine ligands, α-ketoglutarate, water (blue sphere), and a chloride ion (green sphere).[37] $2F_o - F_c$ electron density maps are shown in blue mesh and contoured at 1.0σ. (B.) A dispersive difference Fourier map from a SyrB2 crystal that contained bromide (purple sphere).[37] This map, calculated by subtracting data collected at the iron edge (1.7340 Å) from data collected at the bromide edge (0.9197 Å), shows a positive density peak for bromine (purple mesh contoured at 4.0σ), and a negative density peak for iron (brown mesh contoured at −4.0σ) due to the differential scattering of these two ions at these wavelengths. Panel B was reprinted from ref 37.

Phase Determination

Metal centers within a protein provide a native way to determine phase information with single-wavelength anomalous dispersion (SAD) or multiwavelength anomalous dispersion (MAD) experiments, techniques that have become mainstream with increased availability of wavelength-tunable synchrotron facilities. For both *S*-adenosylmethionine radical enzymes, anaerobic sulfatase maturating enzyme (anSME) from *Clostridium perfringens* and 7-carboxy-7-deazaguanine synthase (QueE) from *Burkholderia multivorans*, phases were determined by SAD methods with data collected from a rotating copper anode home source at the Cu Kα edge (1.54178 Å).[29,32] The enzyme anSME has three [4Fe−4S] clusters per monomer, and QueE has one [4Fe−4S] cluster per monomer (Figure 4A,B).[29,32] Both structures show the utility of the incorporated [4Fe−4S] clusters; because there is significant iron anomalous signal at the Cu Kα edge, the presence of the metallocofactor allowed phases to be obtained and structures to be solved from a home source (Figure 4C).

Another option to determine or improve phases for metalloprotein structures is to use the wavelength dependence of X-ray diffraction (known as dispersive differences) for the given metal and collect data using a tunable synchrotron beamline. The structures of biotin synthase and pyruvate formate-lyase activating enzyme, both of which contain Fe−S clusters, were determined to 2.25 Å and 3.4 Å resolution using iron MAD techniques.[30,31] The phasing power of incorporated metalloclusters not only pertains to iron; a recent example of phasing from the incorporated metallocofactor is the crystal structure of CarH, a photoreceptor that uses one molecule of AdoCbl per monomer as a light-dependent switch to mediate transcription regulation.[52] The structure of the light-sensing domains of CarH was solved using data collected at the cobalt peak wavelength (1.6039 Å), and a SAD experiment was used to locate the cobalt of AdoCbl (Figure 5).[52] Of course, there are many examples where phasing off the metal center alone was not sufficient to solve the phase problem and other methods were needed. For example, the structure of benzylsuccinate synthase, which has two intact [4Fe−4S] clusters per heterohexamer (228 kDa), could not be solved

DOI: 10.1021/acs.accounts.5b00538
Acc. Chem. Res. 2016, 49, 695−702

Table 2. Optical Properties of Some Protein Bound Metal Centers

metal	example protein	redox state	optical properties	"main" peaks (nm)	ε (M^{-1} cm^{-1})
cobalt	methionine synthase[47]	Co(III)	strong	352	20200
		Co(II)	strong	475	9470
		Co(I)	strong	525	10000
iron (heme)	cyt c[48]	Fe(III)	strong	410	100000
		Fe(II)	strong	413, 521, 550	125000, 1550, 2900
iron (Fe−S)	rubredoxin[49]	Fe(III)	strong	350, 380, 490	7000, 7700, 6600
		Fe(II)	silent		
copper	nitrite reductase[50]	type I Cu(II)	strong	600	2880
nickel	nickel superoxide dismutase[51]	Ni(III)	strong	378	6000
		Ni(II)	weak	450	<500

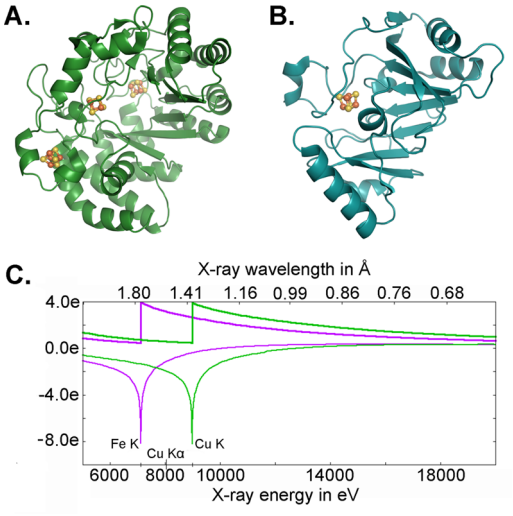

Figure 4. Data collected at the Cu Kα edge can be used to determine phases for Fe−S cluster containing protein structures. The crystal structures of (A) anSME[29] and (B) QueE[32] were solved using the anomalous signal of protein-bound [4Fe−4S] clusters and data collected at the Cu Kα edge. (C) Calculated anomalous scattering at the Fe and Cu K edge. Plot generated with edgeplots web tool from http://skuld.bmsc.washington.edu/scatter/.

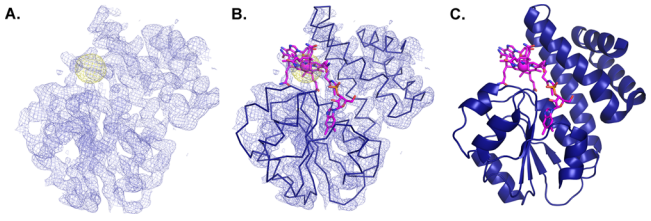

Figure 5. Bound metallocofactor AdoCbl is exploited for phase information in CarH. The crystal structure of two domains of the AdoCbl-dependent transcription factor, CarH, was solved using anomalous scattering of the cobalt ion.[52] (A) Experimental electron density maps contoured at 1.2σ (purple) and anomalous electron density map contoured at 5.0σ (yellow). (B) Ribbon trace of AdoCbl, the Cbl-binding and helix bundle domains built into the electron density. (C) Resulting structure of the C-terminal light sensing domains of CarH.[52]

using iron anomalous data, and Se-SAD was instead used to determine phase information.[53] To determine the structure of the bifunctional CODH/acetyl-CoA synthase (310 kDa), MAD phasing from the native clusters was combined with molecular replacement phases, subject to multicrystal averaging and 4-fold noncrystallographic symmetry averaging.[54]

Identification of Metals Present

There are a number of different ways to identify which metal ions are present in a crystal, including dispersive difference maps (shown in Figure 3B for SyrB2) and EDX. Recently, EDX was used on calprotectin (CP), an immune response protein that coordinates transition metal ions in a calcium-dependent manner. CP chelates and sequesters metals, functionally depleting the supply of these metals for use by pathogens.[55,56]

In a recently determined structure of Mn(II)Ca(II)CP, anomalous maps showed density consistent with Mn^{2+} in the Mn^{2+}-binding site, but Ca^{2+} in only one of the two proposed Ca^{2+}-binding sites, raising questions of how many Ca^{2+}-binding sites are really there (Figure 6A).[57] EDX experiments were also

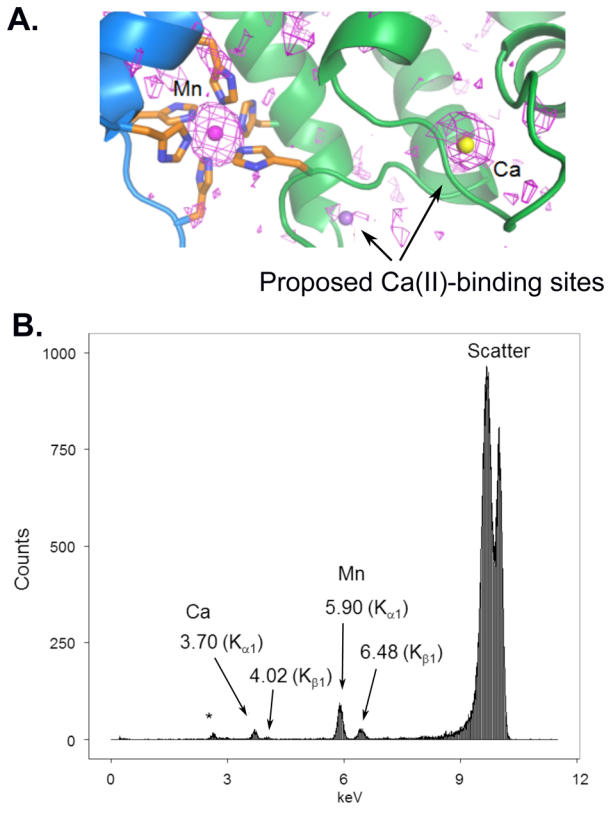

Figure 6. A number of techniques can be used to identify metals within metalloprotein crystals. (A) Anomalous maps (1.54178 Å) contoured at 2.0σ are consistent with Mn^{2+} in the Mn^{2+} site and Ca^{2+} in only one of the two expected calcium-binding sites shown in CP.[57] (B) EDX spectrum of a Mn(II)Ca(II)-bound CP indicates presence of both metals (* indicates presence of K^+). Panel A was reprinted from ref 57.

DOI: 10.1021/acs.accounts.5b00538
Acc. Chem. Res. 2016, 49, 695−702

performed on single crystals of CP bound to a variety of metals, illustrating the use of EDX to verify the presence and identity of metals within a single crystal (Figure 6B).

Clarification of Proposed Reaction Mechanisms

Copper-containing nitrite reductases (CuNiRs) catalyze formation of nitric oxide from reduction of nitrite, an important step in denitrification.[18] CuNiRs contain two copper centers (Cu-center): a type I copper site involved in electron transfer and a type II copper site for binding nitrite. A combination of X-ray crystallography and spectroscopic experiments on CuNiR from *Alcaligenes xylosoxidans* (AxNiR) provided support for an ordered mechanism for electron transfer in CuNiRs. UV−vis spectroscopy on the CuNiR blue crystal indicated that the type I Cu center is in the Cu^{2+} oxidation state prior to X-ray exposure but becomes reduced after data collection (Figure 7).[18] EXAFS was used to investigate the oxidation state of the

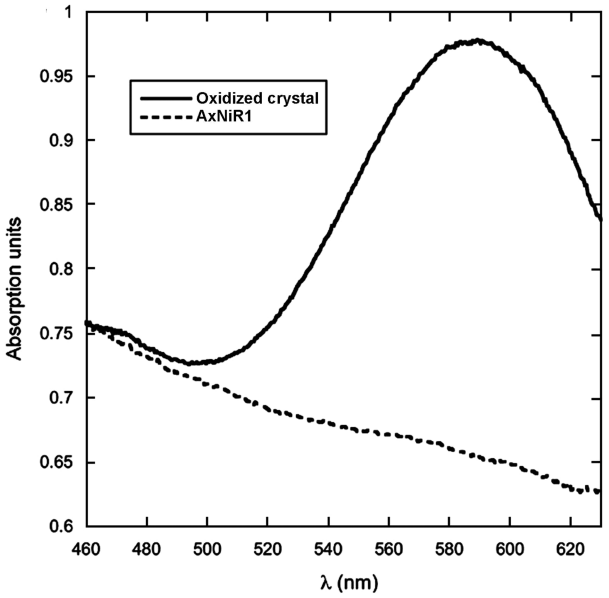

Figure 7. Parallel UV−vis spectroscopy and X-ray crystallography lend support to an ordered mechanism proposed for AxNiR. The intense peak at 595 nm is characteristic of a type I Cu^{2+} site and disappears after exposure to X-rays, consistent with reduction.[18] Reproduced with permission from ref 18. Copyright 2008 Elsevier Ltd.

type II Cu center, revealing that, in the absence of nitrite, this site remains oxidized.[18] These results give strong evidence for the proposed ordered mechanism, in which the type I Cu center transfers an electron to the type II Cu center to catalyze the reaction, when the substrate is bound.[18]

Determination of Crystallized Protein Activity

A fundamental challenge in the interpretation of protein crystallographic data is unawareness about whether the structure represents an active or inactive state of the enzyme. For crystals with optically active metals, microspectrophotometry allows assessment of whether the exact structure observed crystallographically is catalytically active. In a study of CFeSP/methyl transferase (MeTr) complex from *M. thermoacetica*, microspectrophotometry was used to show that crystals of the metalloprotein complex were active (Figure 8), an incredible result given that the structure revealed the need for a 17 Å movement of the Cbl-binding domain of CFeSP to get close enough to the methyltetrahydrofolate-binding site on the MeTr

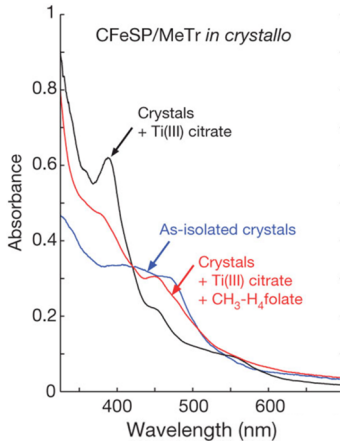

Figure 8. UV−vis of the CFeSP/MeTr crystals show that crystalline protein is active.[15] The spectrum of the CFeSP/MeTr (as-isolated) crystal has features at ∼400 and 470 nm, corresponding to the [4Fe−4S] cluster and Cbl cofactor.[15] Reducing the crystal with Ti(III)-citrate yields a sharp peak at 390 nm, consistent with active Co(I)−Cbl.[15] Addition of CH_3−H_4folate results in a decrease at 390 nm and a new peak at 450 nm, characteristic of product complex for protein-bound CH_3−Co(III).[15] Figure is reprinted from ref 15.

for methyl transfer.[15] This long distance could have meant that the structure was of an inactive state, but instead these spectroscopic data showed *in crystallo* methylation, indicating that the conformation of the enzyme observed in the crystal structure was "on pathway".[15]

SUMMARY

The prevalence of metals and metallocofactors in proteins speaks to the importance of understanding how they are used in biochemical reactions. Recent advances implemented at synchrotron facilities, including incorporation of spectroscopic equipment and detectors that allow simultaneous experiments on single crystals, provides a wealth of new information that can be coupled with the crystallographic structures, revealing details that may otherwise be impossible or difficult to resolve. Although these methods are outside of the scope of this Account, further exciting developments include X-ray free electron laser (XFEL) sources, which produce very short, bright X-ray pulses that effectively outrun radiation damage and oxidation state changes.

AUTHOR INFORMATION

Corresponding Author

*E-mail: cdrennan@mit.edu.

Author Contributions

⊥S.E.J.B. and J.B.-R. contributed equally.

Funding

This work was supported by the National Institutes of Health Grants GM069857 (C.L.D.), F32-GM108189 (J.B.-R.), and F32-GM099257 (S.E.J.B.). C.L.D. is a Howard Hughes Medical Institute Investigator.

Notes

The authors declare no competing financial interest.

Biographies

Sarah Bowman is an HHMI postdoctoral research associate in the Department of Chemistry at the Massachusetts Institute of

DOI: 10.1021/acs.accounts.5b00538
Acc. Chem. Res. 2016, 49, 695−702

Technology (MIT). She studied Chemistry at Metropolitan State College of Denver (B.S., 2005) and at the University of Rochester (Ph.D., 2010), working in the laboratory of Professor Kara Bren. She joined the laboratories of Professors Catherine Drennan and Collin Stultz in 2010 and has been supported by a NIH F32 fellowship. Her research focuses on crystallographic and spectroscopic characterization of metalloproteins.

Jennifer Bridwell-Rabb is an NIH postdoctoral Fellow at MIT. She received three B.S. degrees in Chemistry, Biology, and Mathematics from Central Michigan University in 2007 and her Ph.D. in Chemistry from Texas A&M University in 2012. After graduation, Jennifer joined the laboratory of Professor Catherine Drennan at MIT as an HHMI postdoctoral research associate. Jennifer's research interests include using a combination of enzymology, biophysical approaches, and X-ray crystallography to understand how metalloproteins function in biosynthetic pathways.

Catherine L. Drennan is a professor of Biology and Chemistry at MIT, and a professor and investigator with the Howard Hughes Medical Institute. She received an A.B. in chemistry from Vassar College and a Ph.D. in biological chemistry from the University of Michigan, working in the laboratory of the late Professor Martha L. Ludwig. She was a postdoctoral fellow with Professor Douglas C. Rees at the California Institute of Technology. In 1999, she joined the faculty at MIT, where she has risen through the ranks to full Professor. Cathy's research interests lie at the interface of chemistry and biology. Her laboratory combines X-ray crystallography with other biophysical methods in order to "visualize" molecular processes by obtaining snapshots of metalloproteins in action.

■ ACKNOWLEDGMENTS

We thank Marco Jost and Percival Yang-Ting Chen for Figure 1 photos.

■ REFERENCES

(1) Zheng, H.; Chruszcz, M.; Lasota, P.; Lebioda, L.; Minor, W. Data mining of metal ion environments present in protein structures. *J. Inorg. Biochem.* **2008**, *102*, 1765−1776.
(2) Waldron, K. J.; Rutherford, J. C.; Ford, D.; Robinson, N. J. Metalloproteins and metal sensing. *Nature* **2009**, *460*, 823−830.
(3) Lippard, S. J.; Berg, J. M. *Principles of Bioinorganic Chemistry*; University Science Books: Mill Valley, CA, 1994.
(4) Rosenzweig, A. C. Metallochaperones: bind and deliver. *Chem. Biol.* **2002**, *9*, 673−677.
(5) Zheng, L.; Cash, V. L.; Flint, D. H.; Dean, D. R. Assembly of iron-sulfur clusters. Identification of an iscSUA-hscBA-fdx gene cluster from Azotobacter vinelandii. *J. Biol. Chem.* **1998**, *273*, 13264−13272.
(6) Posewitz, M. C.; King, P. W.; Smolinski, S. L.; Zhang, L.; Seibert, M.; Ghirardi, M. L. Discovery of two novel radical S-adenosylmethionine proteins required for the assembly of an active [Fe] hydrogenase. *J. Biol. Chem.* **2004**, *279*, 25711−25720.
(7) Jacobson, M. R.; Cash, V. L.; Weiss, M. C.; Laird, N. F.; Newton, W. E.; Dean, D. R. Biochemical and genetic analysis of the nifUSVWZM cluster from Azotobacter vinelandii. *Mol. Gen. Genet.* **1989**, *219*, 49−57.
(8) Kerby, R. L.; Ludden, P. W.; Roberts, G. P. In vivo nickel insertion into the carbon monoxide dehydrogenase of Rhodospirillum rubrum: molecular and physiological characterization of cooCTJ. *J. Bacteriol.* **1997**, *179*, 2259−2266.
(9) Kim, J.; Rees, D. C. Structural models for the metal centers in the nitrogenase molybdenum-iron protein. *Science* **1992**, *257*, 1677−1682.
(10) Burger, E. M.; Andrade, S.; Einsle, O. Active sites without restraints: high-resolution analysis of metal cofactors. *Curr. Opin. Struct. Biol.* **2015**, *35*, 32−40.
(11) Einsle, O.; Tezcan, F. A.; Andrade, S. L.; Schmid, B.; Yoshida, M.; Howard, J. B.; Rees, D. C. Nitrogenase MoFe-protein at 1.16 A resolution: a central ligand in the FeMo-cofactor. *Science* **2002**, *297*, 1696−1700.
(12) Hu, Y.; Ribbe, M. W. A journey into the active center of nitrogenase. *JBIC, J. Biol. Inorg. Chem.* **2014**, *19*, 731−736.
(13) Spatzal, T.; Aksoyoglu, M.; Zhang, L.; Andrade, S. L.; Schleicher, E.; Weber, S.; Rees, D. C.; Einsle, O. Evidence for interstitial carbon in nitrogenase FeMo cofactor. *Science* **2011**, *334*, 940.
(14) Lancaster, K. M.; Roemelt, M.; Ettenhuber, P.; Hu, Y.; Ribbe, M. W.; Neese, F.; Bergmann, U.; DeBeer, S. X-ray emission spectroscopy evidences a central carbon in the nitrogenase iron-molybdenum cofactor. *Science* **2011**, *334*, 974−977.
(15) Kung, Y.; Ando, N.; Doukov, T. I.; Blasiak, L. C.; Bender, G.; Seravalli, J.; Ragsdale, S. W.; Drennan, C. L. Visualizing molecular juggling within a B12-dependent methyltransferase complex. *Nature* **2012**, *484*, 265−269.
(16) Yano, J.; Kern, J.; Irrgang, K. D.; Latimer, M. J.; Bergmann, U.; Glatzel, P.; Pushkar, Y.; Biesiadka, J.; Loll, B.; Sauer, K.; Messinger, J.; Zouni, A.; Yachandra, V. K. X-ray damage to the Mn4Ca complex in single crystals of photosystem II: a case study for metalloprotein crystallography. *Proc. Natl. Acad. Sci. U. S. A.* **2005**, *102*, 12047−12052.
(17) Einsle, O.; Andrade, S. L.; Dobbek, H.; Meyer, J.; Rees, D. C. Assignment of individual metal redox states in a metalloprotein by crystallographic refinement at multiple X-ray wavelengths. *J. Am. Chem. Soc.* **2007**, *129*, 2210−2211.
(18) Hough, M. A.; Antonyuk, S. V.; Strange, R. W.; Eady, R. R.; Hasnain, S. S. Crystallography with online optical and X-ray absorption spectroscopies demonstrates an ordered mechanism in copper nitrite reductase. *J. Mol. Biol.* **2008**, *378*, 353−361.
(19) Ronda, L.; Bruno, S.; Bettati, S.; Storici, P.; Mozzarelli, A. From protein structure to function via single crystal optical spectroscopy. *Front. Mol. Biosci.* **2015**, *2*, 12.
(20) Antonyuk, S. V.; Hough, M. A. Monitoring and validating active site redox states in protein crystals. *Biochim. Biophys. Acta, Proteins Proteomics* **2011**, *1814*, 778−784.
(21) De la Mora-Rey, T.; Wilmot, C. M. Synergy within structural biology of single crystal optical spectroscopy and X-ray crystallography. *Curr. Opin. Struct. Biol.* **2007**, *17*, 580−586.
(22) Orville, A. M.; Buono, R.; Cowan, M.; Heroux, A.; Shea-McCarthy, G.; Schneider, D. K.; Skinner, J. M.; Skinner, M. J.; Stoner-Ma, D.; Sweet, R. M. Correlated single-crystal electronic absorption spectroscopy and X-ray crystallography at NSLS beamline X26-C. *J. Synchrotron Radiat.* **2011**, *18*, 358−366.
(23) Cotelesage, J. J.; Pushie, M. J.; Grochulski, P.; Pickering, I. J.; George, G. N. Metalloprotein active site structure determination: synergy between X-ray absorption spectroscopy and X-ray crystallography. *J. Inorg. Biochem.* **2012**, *115*, 127−137.
(24) Kekilli, D.; Dworkowski, F. S.; Pompidor, G.; Fuchs, M. R.; Andrew, C. R.; Antonyuk, S.; Strange, R. W.; Eady, R. R.; Hasnain, S. S.; Hough, M. A. Fingerprinting redox and ligand states in haemprotein crystal structures using resonance Raman spectroscopy. *Acta Crystallogr., Sect. D: Biol. Crystallogr.* **2014**, *70*, 1289−1296.
(25) Stoner-Ma, D.; Skinner, J. M.; Schneider, D. K.; Cowan, M.; Sweet, R. M.; Orville, A. M. Single-crystal Raman spectroscopy and X-ray crystallography at beamline X26-C of the NSLS. *J. Synchrotron Radiat.* **2011**, *18*, 37−40.
(26) Kirn, J.; Rees, D. C. Crystallographic structure and functional implications of the nitrogenase molybdenum-iron protein from azotobacter vinelandii. *Nature* **1992**, *360*, 553−560.
(27) Drennan, C. L.; Heo, J.; Sintchak, M. D.; Schreiter, E.; Ludden, P. W. Life on carbon monoxide: X-ray structure of Rhodospirillum rubrum Ni-Fe-S carbon monoxide dehydrogenase. *Proc. Natl. Acad. Sci. U. S. A.* **2001**, *98*, 11973−11978.
(28) Goldman, P. J.; Grove, T. L.; Booker, S. J.; Drennan, C. L. X-ray analysis of butirosin biosynthetic enzyme BtrN redefines structural motifs for AdoMet radical chemistry. *Proc. Natl. Acad. Sci. U. S. A.* **2013**, *110*, 15949−15954.

DOI: 10.1021/acs.accounts.5b00538
Acc. Chem. Res. 2016, 49, 695−702

(29) Goldman, P. J.; Grove, T. L.; Sites, L. A.; McLaughlin, M. I.; Booker, S. J.; Drennan, C. L. X-ray structure of an AdoMet radical activase reveals an anaerobic solution for formylglycine posttranslational modification. *Proc. Natl. Acad. Sci. U. S. A.* **2013**, *110*, 8519−8524.
(30) Berkovitch, F.; Nicolet, Y.; Wan, J. T.; Jarrett, J. T.; Drennan, C. L. Crystal structure of biotin synthase, an S-adenosylmethionine-dependent radical enzyme. *Science* **2004**, *303*, 76−79.
(31) Vey, J. L.; Yang, J.; Li, M.; Broderick, W. E.; Broderick, J. B.; Drennan, C. L. Structural basis for glycyl radical formation by pyruvate formate-lyase activating enzyme. *Proc. Natl. Acad. Sci. U. S. A.* **2008**, *105*, 16137−16141.
(32) Dowling, D. P.; Bruender, N. A.; Young, A. P.; McCarty, R. M.; Bandarian, V.; Drennan, C. L. Radical SAM enzyme QueE defines a new minimal core fold and metal-dependent mechanism. *Nat. Chem. Biol.* **2014**, *10*, 106−112.
(33) Esselborn, J.; Muraki, N.; Klein, K.; Engelbrecht, V.; Metzler-Nolte, N.; Apfel, U.-P.; Hofmann, E.; Kurisu, G.; Happe, T. A structural view of synthetic cofactor integration into [FeFe]-hydrogenases. *Chem. Sci.* **2016**, *7*, 959−968.
(34) Imlay, J. A. Pathways of oxidative damage. *Annu. Rev. Microbiol.* **2003**, *57*, 395−418.
(35) Phillips, C. M.; Schreiter, E. R.; Stultz, C. M.; Drennan, C. L. Structural basis of low-affinity nickel binding to the nickel-responsive transcription factor NikR from Escherichia coli. *Biochemistry* **2010**, *49*, 7830−7838.
(36) Sydor, A. M.; Jost, M.; Ryan, K. S.; Turo, K. E.; Douglas, C. D.; Drennan, C. L.; Zamble, D. B. Metal binding properties of Escherichia coli YjiA, a member of the metal homeostasis-associated COG0523 family of GTPases. *Biochemistry* **2013**, *52*, 1788−1801.
(37) Blasiak, L. C.; Vaillancourt, F. H.; Walsh, C. T.; Drennan, C. L. Crystal structure of the non-haem iron halogenase SyrB2 in syringomycin biosynthesis. *Nature* **2006**, *440*, 368−371.
(38) Hope, H. Cryocrystallography of biological macromolecules: a generally applicable method. *Acta Crystallogr., Sect. B: Struct. Sci.* **1988**, *44*, 22−26.
(39) Henderson, R. Cryoprotection of Protein Crystals against Radiation-Damage in Electron and X-Ray-Diffraction. *Proc. R. Soc. London, Ser. B* **1990**, *241*, 6−8.
(40) Ravelli, R. B.; McSweeney, S. M. The 'fingerprint' that X-rays can leave on structures. *Structure* **2000**, *8*, 315−328.
(41) Gonzalez, A.; Nave, C. Radiation damage in protein crystals at low temperature. *Acta Crystallogr., Sect. D: Biol. Crystallogr.* **1994**, *50*, 874−877.
(42) Hersleth, H. P.; Andersson, K. K. How different oxidation states of crystalline myoglobin are influenced by X-rays. *Biochim. Biophys. Acta, Proteins Proteomics* **2011**, *1814*, 785−796.
(43) Champloy, F.; Gruber, K.; Jogl, G.; Kratky, C. XAS spectroscopy reveals X-ray-induced photoreduction of free and protein-bound B12 cofactors. *J. Synchrotron Radiat.* **2000**, *7*, 267−273.
(44) Can, M.; Krucinska, J.; Zoppellaro, G.; Andersen, N. H.; Wedekind, J. E.; Hersleth, H. P.; Andersson, K. K.; Bren, K. L. Structural characterization of nitrosomonas europaea cytochrome c-552 variants with marked differences in electronic structure. *ChemBioChem* **2013**, *14*, 1828−1838.
(45) Zoppellaro, G.; Harbitz, E.; Kaur, R.; Ensign, A. A.; Bren, K. L.; Andersson, K. K. Modulation of the ligand-field anisotropy in a series of ferric low-spin cytochrome c mutants derived from Pseudomonas aeruginosa cytochrome c-551 and Nitrosomonas europaea cytochrome c-552: a nuclear magnetic resonance and electron paramagnetic resonance study. *J. Am. Chem. Soc.* **2008**, *130*, 15348−15360.
(46) Meharenna, Y. T.; Doukov, T.; Li, H.; Soltis, S. M.; Poulos, T. L. Crystallographic and single-crystal spectral analysis of the peroxidase ferryl intermediate. *Biochemistry* **2010**, *49*, 2984−2986.
(47) Jarrett, J. T.; Amaratunga, M.; Drennan, C. L.; Scholten, J. D.; Sands, R. H.; Ludwig, M. L.; Matthews, R. G. Mutations in the B12-binding region of methionine synthase: how the protein controls methylcobalamin reactivity. *Biochemistry* **1996**, *35*, 2464−2475.
(48) Banci, L.; Assfalg, M. Mitochondrial cytochrome c. In *Encyclopedia of Inorganic and Bioinorganic Chemistry*; John Wiley & Sons, Ltd: New York, 2011.
(49) Meyer, J.; Moulis, J.-M. Rubredoxin. In *Encyclopedia of Inorganic and Bioinorganic Chemistry*; John Wiley & Sons, Ltd: New York, 2011.
(50) Ichiki, H.; Tanaka, Y.; Mochizuki, K.; Yoshimatsu, K.; Sakurai, T.; Fujiwara, T. Purification, characterization, and genetic analysis of Cu-containing dissimilatory nitrite reductase from a denitrifying halophilic archaeon, Haloarcula marismortui. *J. Bacteriol.* **2001**, *183*, 4149−4156.
(51) Bryngelson, P.; Maroney, M. Nickel superoxide dismutase. In *Nickel and Its Surprising Impact in Nature*; Sigel, A., Sigel, H., Sigel, R., Eds.; Metal Ions in Life Sciences; John Wiley & Sons, Ltd: Chicester, 2007; Vol. 2.
(52) Jost, M.; Fernandez-Zapata, J.; Polanco, M. C.; Ortiz-Guerrero, J. M.; Chen, P. Y.; Kang, G.; Padmanabhan, S.; Elias-Arnanz, M.; Drennan, C. L. Structural basis for gene regulation by a B12-dependent photoreceptor. *Nature* **2015**, *526*, 536−541.
(53) Funk, M. A.; Judd, E. T.; Marsh, E. N.; Elliott, S. J.; Drennan, C. L. Structures of benzylsuccinate synthase elucidate roles of accessory subunits in glycyl radical enzyme activation and activity. *Proc. Natl. Acad. Sci. U. S. A.* **2014**, *111*, 10161−10166.
(54) Doukov, T. I.; Iverson, T. M.; Seravalli, J.; Ragsdale, S. W.; Drennan, C. L. A Ni-Fe-Cu center in a bifunctional carbon monoxide dehydrogenase/acetyl-CoA synthase. *Science* **2002**, *298*, 567−572.
(55) Brophy, M. B.; Nolan, E. M. Manganese and microbial pathogenesis: sequestration by the Mammalian immune system and utilization by microorganisms. *ACS Chem. Biol.* **2015**, *10*, 641−651.
(56) Becker, K. W.; Skaar, E. P. Metal limitation and toxicity at the interface between host and pathogen. *FEMS Microbiol Rev.* **2014**, *38*, 1235−1249.
(57) Gagnon, D. M.; Brophy, M. B.; Bowman, S. E.; Stich, T. A.; Drennan, C. L.; Britt, R. D.; Nolan, E. M. Manganese binding properties of human calprotectin under conditions of high and low calcium: X-ray crystallographic and advanced electron paramagnetic resonance spectroscopic analysis. *J. Am. Chem. Soc.* **2015**, *137*, 3004−3016.

DOI: 10.1021/acs.accounts.5b00538
Acc. Chem. Res. 2016, 49, 695−702